

# Synthesis and Characterization of the Biodegradable Copolymers from Succinic Acid and Adipic Acid with 1,4-Butanediol

B. D. AHN,<sup>1-3</sup> S. H. KIM,<sup>1,\*</sup> Y. H. KIM,<sup>1</sup> J. S. YANG<sup>2</sup>

<sup>1</sup> Biomaterials Research Center, Korea Institute of Science and Technology (KIST), Seoul, South Korea

<sup>2</sup> Department of Chemistry, Kyung Hee University, Seoul, South Korea

<sup>3</sup> Research Section, Korea Testing and Research Institute for Chemical Industry (KOTRIC), Seoul, South Korea

Received 12 September 2000; accepted 19 February 2001

**ABSTRACT:** Biodegradable homopolyesters such as poly(butylene succinate) (PBSU) and poly(butylene adipate) (PBAD) and copolyesters such as poly(butylene succinate-co-butylene adipate) (PBSA) were synthesized, respectively, from succinic acid (SA) and adipic acid (AA) with 1,4-butanediol through a two-step process of esterification and deglycolization. The polyester compositions and physical properties of both homopolyesters and copolyesters were investigated by <sup>1</sup>H- and <sup>13</sup>C-NMR, DSC, GPC, WAXD, and optical polarizing microscopy. The melting point ( $T_m$ ) of these copolyesters decreased gradually as the contents of butylene adipate increased and the glass-transition temperature ( $T_g$ ) of these copolyesters decreased linearly as the contents of the adipoyl unit increased. PBSA copolyesters showed two types of XRD patterns of PBSU and PBAD homopolyesters. Furthermore, the biodegradation and hydrolytic degradation of the high molecular weight PBSU homopolyester, PBAD homopolyester, and PBSA copolyesters were investigated in the composting soil and NH<sub>4</sub>Cl aqueous solutions at a pH level of 10.6. © 2001 John Wiley & Sons, Inc. *J Appl Polym Sci* 82: 2808–2826, 2001

**Key words:** biodegradable aliphatic polyester; poly(butylene succinate-co-butylene adipate); gel permeation chromatography; differential scanning calorimetry; crystallinity; biodegradation

## INTRODUCTION

Recently, many researchers have worked to develop ecological plastic products because of environmental concerns. Worldwide production of plastics is more than 110 million tons per year. Almost half of them are discarded within a short

time and remained in garbage deposits and landfills for decades. Therefore, synthetic plastics have accumulated in nature at a rate of 25 million tons per year. For this reason, it is necessary to develop more recyclable and/or biodegradable plastics to reduce the amount of plastics in landfills. Biodegradable polymers are already utilized in many biomedical applications, such as biodegradable sutures, wound dressing, bioabsorbable implants, and drug delivery systems where the high cost of the materials is justified.<sup>1-4</sup> However, their uses in commodity applications, such as packaging or agriculture, are still limited because

Correspondence to: S. H. Kim.

\* Present address: Biomaterials Research Center, Korea Institute of Science and Technology (KIST), P.O. Box 131, Cheongryang, Seoul 130-650, South Korea.

*Journal of Applied Polymer Science*, Vol. 82, 2808–2826 (2001)  
© 2001 John Wiley & Sons, Inc.

of economical reasons or difficulties related to their processing.

Among the most interesting biodegradable polymers, aliphatic polyester, polyesteramide, polyestercarbonate, poly(butylene succinate) (PBSU), poly(butylene adipate) (PBAD), and poly(butylene succinate-co-butylene adipate) (PBSA) were commercialized for plastic commodities, films, and agricultural products.<sup>5–10</sup> The biodegradability of these polyesters is sensitive to their structures, crystallinities, molecular weights, hydrophobicities, and so forth.<sup>11,12</sup> Therefore, many investigations are currently being carried out to stimulate the biodegradability of the polyesters by simply modifying their physical properties.

Recently, based on the low molecular weights of PBSU and PBAD, the results of facilitated biodegradation by altering their microstructures, crystal structures, crystallinities, and melting temperatures were reported.<sup>13–19</sup> Song et al.<sup>14</sup> showed that PBSU prepared from both succinic acid and 1,4-butanediol was effectively degraded by fungi and bacteria, and thermal behavior of PBSU was related to its biodegradability. From the studies of crystal structure and morphology of PBSU, Ihn et al.<sup>15</sup> reported that single crystal growth and lamellar thickness of PBSU were increased along with the growth temperature. Furthermore, Albertsson et al.<sup>16</sup> investigated the transition of biodegradation by changing the molecular weight and crystallinity of PBAD. Although there are many reports regarding the relationships between the biodegradabilities of PBSU and PBAD and their physical properties, a few results has been reported for the PBSA copolyester. Therefore, in this study we report the results from the biodegradation of PBSU, PBAD, and PBSA relating to their microstructures, crystallinities, crystal structures, and melting behaviors by means of chemical composition.

## EXPERIMENTAL

### Materials

Succinic acid (SA) and adipic acid (AA) from Dongyang Chemical Co. (South Korea) were used as the dicarboxylic acid source as received. 1,4-Butanediol was purchased from Junsei Chemical Co. (Japan) and used without further purification process. Titanium isopropoxide as catalyst was obtained from Aldrich (Milwaukee, WI). Also, other

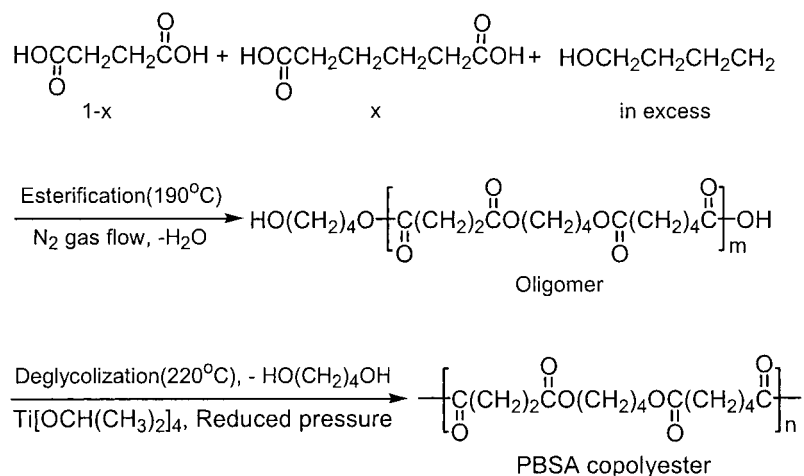
chemicals and solvents were used without further purification.

### Measurements

<sup>1</sup>H- and <sup>13</sup>C-NMR spectra were taken by Bruker ACF-200 (Bruker Instruments, Billerica, MA) using CDCl<sub>3</sub> as a solvent, and the internal standard of chemical shift was TMS. Weight-average molecular weight ( $\overline{M}_w$ ), number-average molecular weight ( $\overline{M}_n$ ), and molecular weight distribution ( $\overline{M}_n/\overline{M}_w$ ) of the resulting polymers were measured by gel permeation chromatography (GPC, Waters 150-C; Waters Instruments, Rochester, MN) equipped with series of columns (Shodex K-801, K-803, K-804, and K-806) and calibrated with polystyrene standards. Eluent solvent was chloroform with a flow rate of 1 mL/min. The concentration of injected sample was 0.5 w/v %. Differential scanning calorimetry (DSC, DuPont TA2100; DuPont, Wilmington, DE) was used to measure the thermal properties of polymers. The heating and cooling were run with 10°C/min under nitrogen atmosphere. The thermal decomposition temperature ( $T_d$ ) was obtained with a heating rate of 20°C/min at a weight loss of 50%. Wide-angle X-ray diffraction (WAXD) for PBSU, PBAD, and PBSA was measured using an X-ray diffractometer (DMAX 2000; Rigaku, Japan) with CuK<sub>α</sub> radiation. An optical polarizing microscope (MPS 32; Leica, Deerfield, IL) was used to observe the spherulitic structure of polymers on a hot plate for 2 min at 150°C then cooled down to room temperature, after which samples were observed under identical conditions. A scanning electron micrograph (SEM, Leica Stereoscan 440; LEO, UK) was used to observe the surface morphology change of the sample, which was obtained during the hydrolytic degradation.

### Synthesis

PBSU and PBAD homopolyesters and PBSA copolyesters were polymerized by setting up a four-neck reaction vessel with mechanical stirrer on a thermosetted oil bath. Succinic acid and adipic acid (0.3 mol) were added into the reactor with various mol ratios. 1,4-Butanediol and dicarboxylic acid were added with a mol ratio of 1 : 1.04–1.10. The temperature was increased slowly until the acid component dissolved completely under N<sub>2</sub> gas. The polymerization consisted of esterification and deglycolization reactions; in the process of esterification, H<sub>2</sub>O (0.6 mol) was collected



**Scheme 1** Synthesis of PBSA copolyesters from succinic acid and adipic acid with 1,4-butanediol.

using a trap device and the reaction was completed in the condition of  $\text{N}_2$  gas flow for 2 h at  $190^\circ\text{C}$ . The active catalyst titanium isopropoxide was added prior to deglycolization. For the deglycolization, the pressure was depressed steadily to below 67 Pa for 6 to 10 h at the reaction temperature of  $220^\circ\text{C}$ . The structures of these copolyesters are presented in **Scheme 1**.

### Degradation

The biodegradable tests of PBSU and PBAD homopolyesters and PBSA copolyesters were carried out by measuring the biological oxygen demand (BOD) inside a closed bottle using the activated-sewage sludge. To standardize the contact surface area, the sample was dissolved in chloroform and poured into cold methanol (volume ratio 1 : 500) to form a cottonlike fiber. Phosphate buffer solution (pH 7.2) was used as the basal medium. According to the guideline for testing of chemicals in the OECD testing method, the BOD can be used for monitoring degradation.<sup>20</sup>

The landfill test was produced by controlling the inside of the automatically controlled incubator that was regulated  $30 \pm 1^\circ\text{C}$  with humidity of 90%. A uniform commercial soil consisting of compost and soil mixture (50 : 50) with initial moisture content of 54.2% and initial pH 7.2 was used as degradation medium. The plastic samples of  $20 \times 20 \times 0.4$  mm were buried in a depth of 5 cm. The landfill test was checked out through the weight loss and surface observations.

The hydrolytic degradation was started by putting a 0.4-mm-thick film in an ammonium chlo-

ride buffer solution (pH 10.6). To prevent the degradation by microorganisms, 0.3 w/v % of  $\text{NaN}_3$  was given as an antibacterial agent and mixed in a shaking incubator at 50 rpm and  $30^\circ\text{C}$ . The degradability was measured through molecular weight change and weight loss. A buffer solution (pH 10.6) was produced by dissolving 67.5 g of  $\text{NH}_4\text{Cl}$  in  $\text{NH}_4\text{OH}$  (570 mL), and then adding to distilled water to be 1 L.

## RESULTS AND DISCUSSION

### Polymer Synthesis

PBSU and PBAD homopolyesters and PBSA copolyesters were synthesized by two-step reactions of esterification and deglycolization. Because of the hydration, at the esterification reaction  $\bar{M}_n$  and  $\bar{M}_w$  exhibited values of 1000 and 2000, respectively. For the deglycolization reaction,  $0.9 \times 10^{-4}$  mol/oligomer of titanium isopropoxide was used as a catalyst under nitrogen atmosphere, and then an oil bath was heated to  $220^\circ\text{C}$ . It was gradually decompressed and finally maintained at a degree of vacuum less than 67 Pa.

Figure 1 shows the  $^{13}\text{C}$ -NMR spectrum of [SA]/[AA] = 79/21 copolyester during esterification at  $190^\circ\text{C}$ . As the adipate and succinate groups of copolyester increase, the peak from succinic acid and adipic acid decreases. This shows that the esterification between monomers progresses as a result of the thermal esterification. The peak of unreacted 1,4-butanediol, added at 1.05–1.10 mol

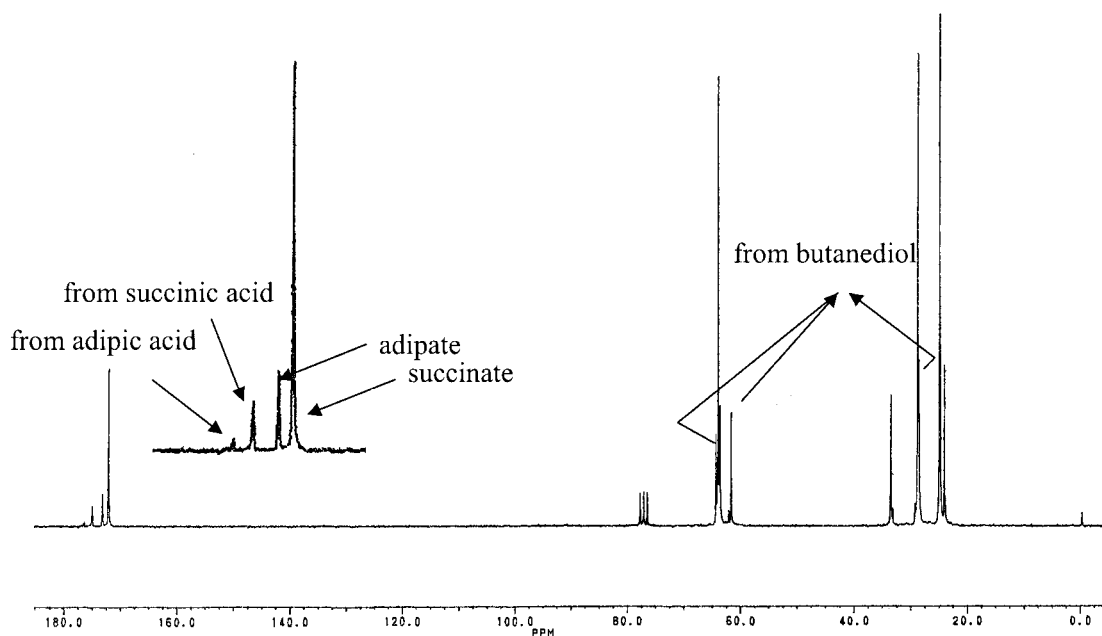


**Figure 1**  $^{13}\text{C}$ -NMR spectrum of the PBSA copolymer ( $[\text{SA}]/[\text{AA}] = 79/21$ ) during the esterification reaction ( $\text{N}_2$  gas flow,  $190^\circ\text{C}$ , 1 h).

ratio to complete the molar equivalent reaction between dicarboxylic acid and diol, disappeared as the deglycolization progressed because of the reduced pressure at the second step of the reac-

tion. PBAD homopolymer needs a longer reaction time compared to that of PBSU homopolymer because of the lower reactivity with 1,4-butanediol.<sup>21</sup>

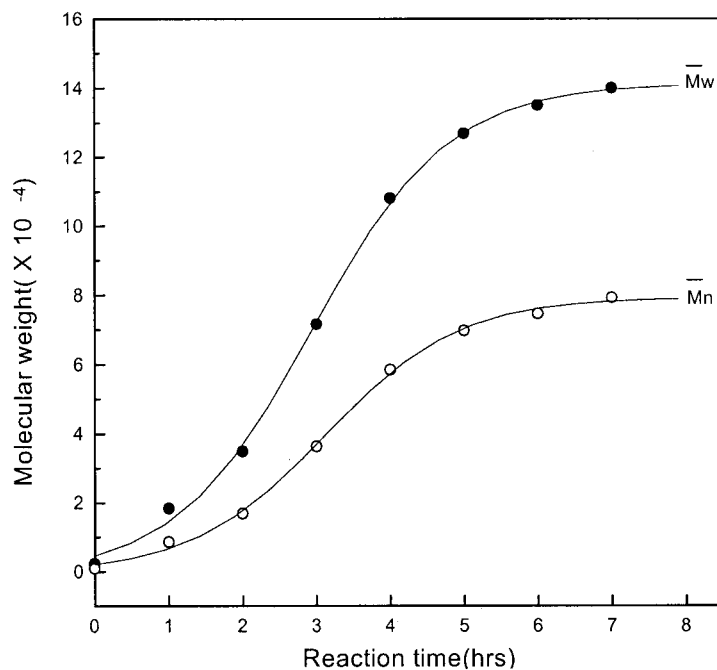


**Figure 2** Results from the polymerization of PBSA copolymer ( $[\text{SA}]/[\text{AA}] = 79/21$ ) during deglycolization reaction at  $220^\circ\text{C}$  with titanium isopropoxide ( $0.9 \times 10^{-4}$  mol/oligomer).

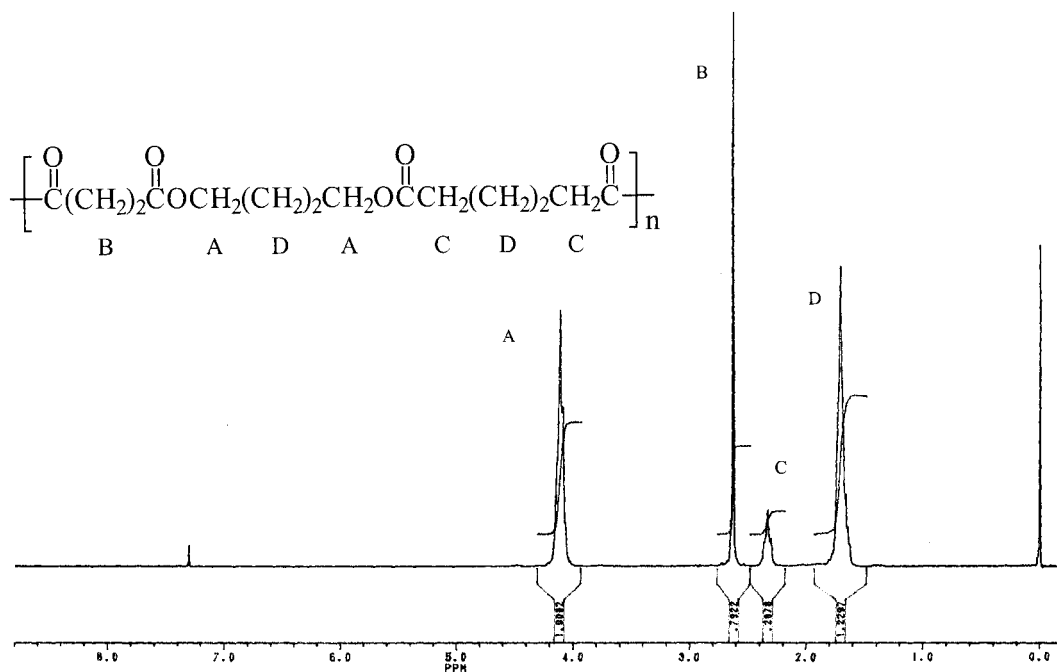


Figure 3 200-MHz  $^1\text{H}$ -NMR spectrum of the PBSA copolyester ([SA]/[AA] = 79/21).

The PBSA copolymer ([SA]/[AA] = 79/21) was characterized by GPC during the deglycolization step. The results are shown in Figure 2, with various molecular weights as a function of reaction times. During the initial 1 to 5 h of reduced pressure,  $\bar{M}_n$  and  $\bar{M}_w$  increased linearly, whereas  $\bar{M}_n/\bar{M}_w$  decreased from 2.6 to 1.8, and the molec-

ular weight increased to  $\bar{M}_w = 140,000$  ( $\bar{M}_n = 79,000$ ) with a narrow molecular weight distribution of 1.78.

#### Polymer Characterization

$^1\text{H}$ - and  $^{13}\text{C}$ -NMR spectra of the PBSA copolyester ([SA]/[AA] = 79/21) are shown, respectively, in

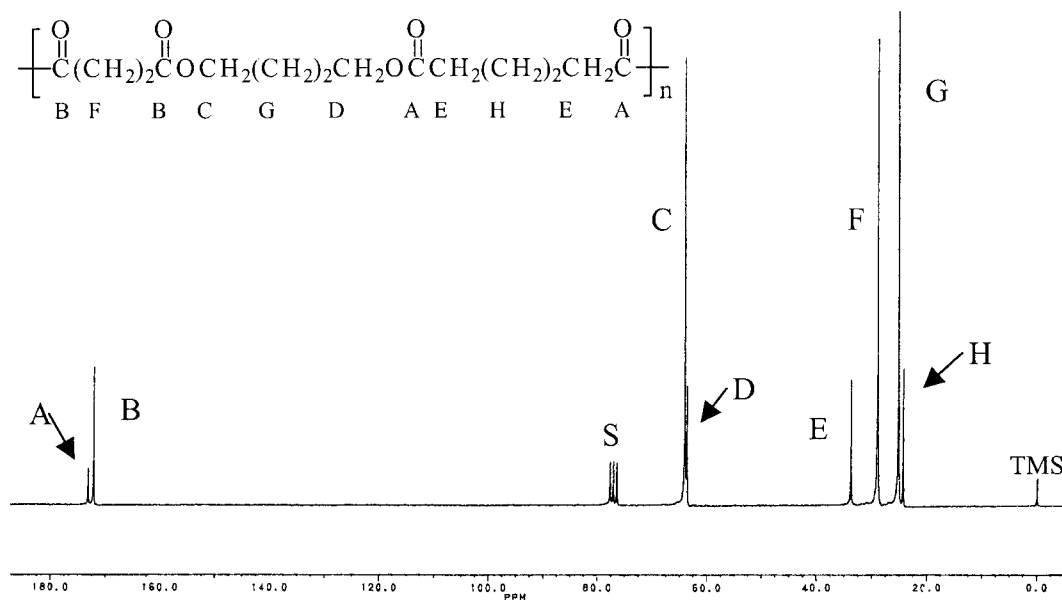


Figure 4 50-MHz  $^{13}\text{C}$ -NMR spectrum of the PBSA copolyester ([SA]/[AA] = 79/21).

**Table I** Copolymerization of Various SA/AA Compositions with 1,4-Butanediol in Bulk at 220°C, 8 h

Run	Composition		Molecular Weight <sup>a</sup>			Thermal Properties			
	Feed Ratio [SA]/[AA]	Polymer Ratio <sup>b</sup> [SA]/[AA]	$\bar{M}_n$ ( $\times 10^{-4}$ )	$\bar{M}_w$ ( $\times 10^{-4}$ )	$\bar{M}_w/\bar{M}_n$	$T_m$ (°C)	$\Delta H_f$ (J/g)	$T_g^c$ (°C)	$T_d^d$ (50 wt %)
PBSU	100/0	100/0	7.7	14.1	1.83	114	70	-33	404
PBSA8/2	80/20	79/21	9.2	16.4	1.78	92	42	-44	399
PBSA6/4	60/40	59/41	9.1	16.1	1.78	65	29	-50	388
PBSA5/5	50/50	51/49	8.9	15.9	1.79	50	28	-51	392
PBSA4/6	40/60	38/62	9.0	16.0	1.78	32	34	-56	388
PBSA2/8	20/80	20/80	7.8	14.2	1.81	46	39	-58	385
PBAD	0/100	0/100	6.2	11.7	1.89	60	53	-60	391

Reaction conditions: succinic acid/adipic acid, 1,4-butanediol, catalyst  $\text{Ti}[\text{OCH}(\text{CH}_3)_2]_4$   $0.9 \times 10^{-4}$  mol/oligomer, temperature 160–220°C, final degree of vacuum 27–67 Pa.

<sup>a</sup> Measured by GPC with chloroform as the eluent and polystyrene standards.

<sup>b</sup> Composition measured by <sup>1</sup>H-NMR.

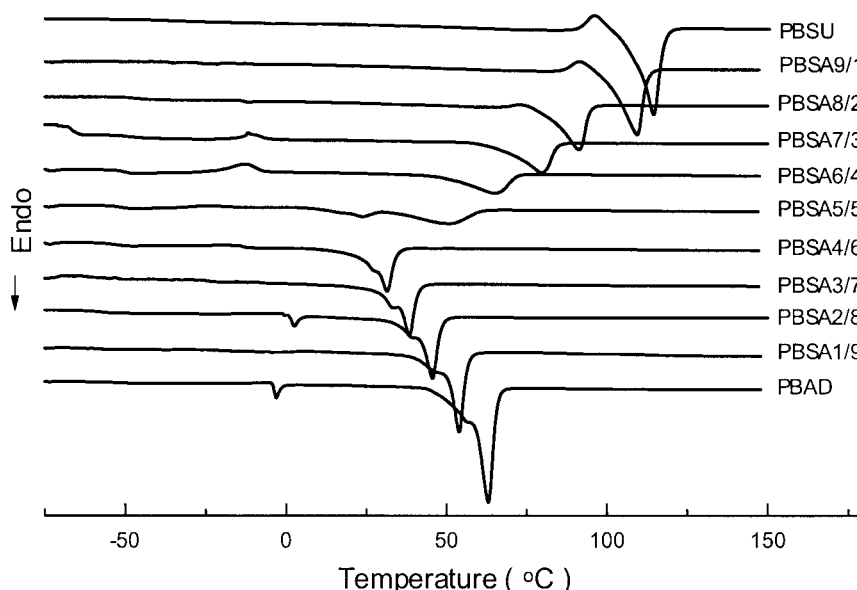
<sup>c</sup> DSC at a heating rate of 10°C/min.

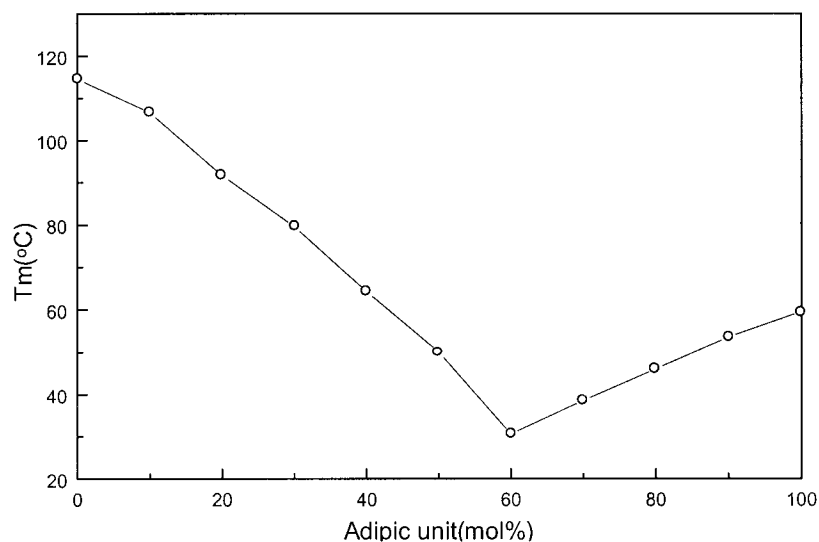
<sup>d</sup> TGA at a heating rate of 20°C/min.

Figure 3 and Figure 4. The <sup>1</sup>H-NMR spectrum of the PBSA copolymer is shown: O—CH<sub>2</sub>—, from the 1,4-butanediol unit at  $\delta$  4.1; COCH<sub>2</sub>—, from the succinyl unit at  $\delta$  2.6; COCH<sub>2</sub>—, from the adipoyl unit at  $\delta$  2.3; and —CH<sub>2</sub>—, from the 1,4-butanediol unit and the adipoyl unit at  $\delta$  1.7. The molar composition of PBSA copolymer was measured as the area ratio of  $\delta$  2.6 peak and  $\delta$  2.3 peak. The <sup>13</sup>C-NMR spectrum is shown: O—CH<sub>2</sub>—, from the 1,4-butanediol unit at  $\delta$  64.2; O—CH<sub>2</sub>—, from the 1,4-butanediol unit at  $\delta$  63.8; —CH<sub>2</sub>—, from the 1,4-butanediol unit at  $\delta$  25.2; —CO, from

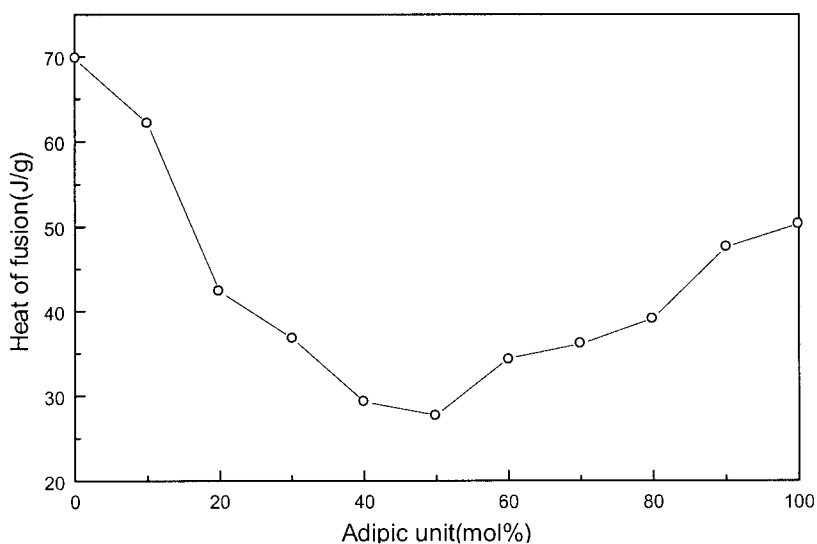
the succinyl unit at  $\delta$  172.3; COCH<sub>2</sub>—, from the succinyl unit at  $\delta$  29.9; —CO, from the adipoyl unit at  $\delta$  173.3; COCH<sub>2</sub>—, from the adipoyl unit at  $\delta$  33.9; and —CH<sub>2</sub>—, from the adipoyl unit at  $\delta$  24.4. They are identical to the signals of PBSU and PBAD homopolyesters.

Copolyester prepared by molten-state polycondensation has generally been considered to have a random distribution of the structural units because of the almost equal reactivities of the monomers and the random transesterification reaction during the polycondensation process. The <sup>13</sup>C-

**Figure 5** DSC thermogram of the PBSA copolymers.



(a)



(b)

**Figure 6** (a) Melting point ( $T_m$ ) and (b) heat of fusion ( $\Delta H_f$ ) for PBSA copolymers measured by DSC.

NMR spectra of all copolyesters were measured in chloroform, and relationships between the structure of the monomeric units and the chemical shifts of the carbonyl,  $\text{O}-\text{CH}_2-$ , and  $-\text{CH}_2-$  signals were established.

Succinic acid and adipic acid were reacted with one diol. This means that the resulting copolyesters contain only two different kinds of ester linkage. In this case, the ratio of these different ester groups depends exclusively on the ratio of the monomers,

although the  $^{13}\text{C}$ -NMR spectrum of such copolyester is identical with that of a mixture of the two corresponding homopolyesters (Fig. 4). However, in the case of aromatic copolyesters, the carbonyl signals are more useful for the analysis of sequence distribution because the aromatic signals are sensitive to the neighboring residue effect.<sup>22-24</sup>

Table I shows the polymer composition, molecular weight, and thermal properties from the copolymerization of various SA/AA compositions

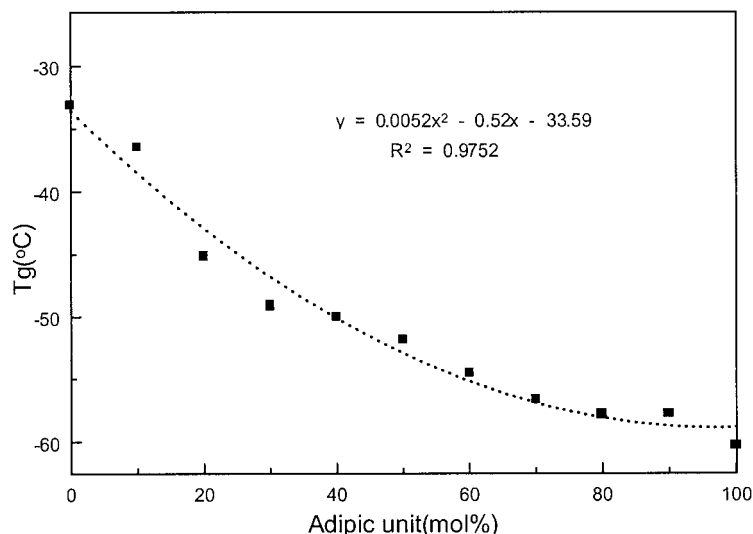


**Figure 7** Glass-transition temperature ( $T_g$ ) for PBSA copolymers measured by DSC.

with 1,4-butanediol in bulk at 220°C. Copolymerization was done as the feed ratio of adipic acid was successively increased by 10 mol %, and the composition ratio of copolyesters was obtained by the integration of methyl proton on the  $^1\text{H-NMR}$  spectrum.

The feed composition and the polymer composition did not show any particular differences but, because of the high boiling point of adipic acid, the composition of the adipate unit became slightly higher. The  $\overline{M}_w$  values of the synthesized PBSA copolyesters, PBSU, and PBAD homopolyester were above 100,000 with a molecular weight distribution of 1.8, which is narrower than those of the conventional condensation copolymers.<sup>25,26</sup>

According to the composition of copolyesters, the melting temperature, melting heat of fusion, glass-transition temperature, and thermal decomposition temperature (50 wt %) were analyzed using DSC and TGA. The copolyesters synthesized from this study are highly crystalline and the  $T_m$ 's of the homopolyester showed at 114 and 60°C, respectively. They showed a tendency to decrease to 32°C as the composition of copolymers increased. Also,  $\Delta H_f$  showed a heat of fusion of the highly crystalline polyester with a similar tendency to  $T_m$ .  $T_g$  was between -33 and 60°C, and decreased linearly as the composition of the adipoyl unit increased. The  $T_d$  monitored at 50 wt % of the sample weight loss was between 404 and 385°C. As a result of the copolymerization they did not show a clear thermal stabilization compared to that of the homopolyester.

The thermal properties of PBSU homopolyester, PBAD homopolyester, and PBSA copolyesters

were measured by DSC/TGA. To look into the thermal history by DSC, all samples were melted isothermally at 150°C, and then the thermal stress was minimized by quenching below the glass-transition temperature. The temperature was then increased at the rate of 10°C/min, and Figure 5 shows the DSC thermogram of these copolymers.  $T_g$  and  $T_m$  of PBSU homopolyester were -33 and 114°C, respectively, and values for PBAD homopolyester were -60 and 60°C, respectively, whereas PBSA copolyesters showed multiple endotherms.

Figure 6(a) shows that as the succinate unit and adipate unit are copolymerized, the melting point attributed to the copolymerization decreased to 62 mol % adipate unit. In addition, as the adipate unit increased more than 62 mol %, the melting point increased, and the typical double-melting endotherm of the thermoplastic polymers did not occur. This was confirmed by modulated DSC analysis.<sup>27-31</sup> As seen in Figure 6(b), the heat of fusion ( $\Delta H_f$ ), the integral value of melting endotherm of DSC first heating, is 70 J/g for PBSU homopolyester, 53 J/g for PBAD homopolyester, and 62-28 J/g for PBSA copolyesters. Under the assumption that the two crystal units participate in the melting behavior of copolymer the cocrystallization between the two units does not occur, and  $\Delta H_f$  decreases according to the copolymerization. As seen in Figure 7, the  $T_g$  of PBSA copolyesters decreases rapidly as the adipate unit in the PBSU homopolyester increased, showing a similar linearity to the general  $T_g$  behavior of random copolymer.<sup>33</sup> It can be concluded that as the succinate unit and adipate unit of



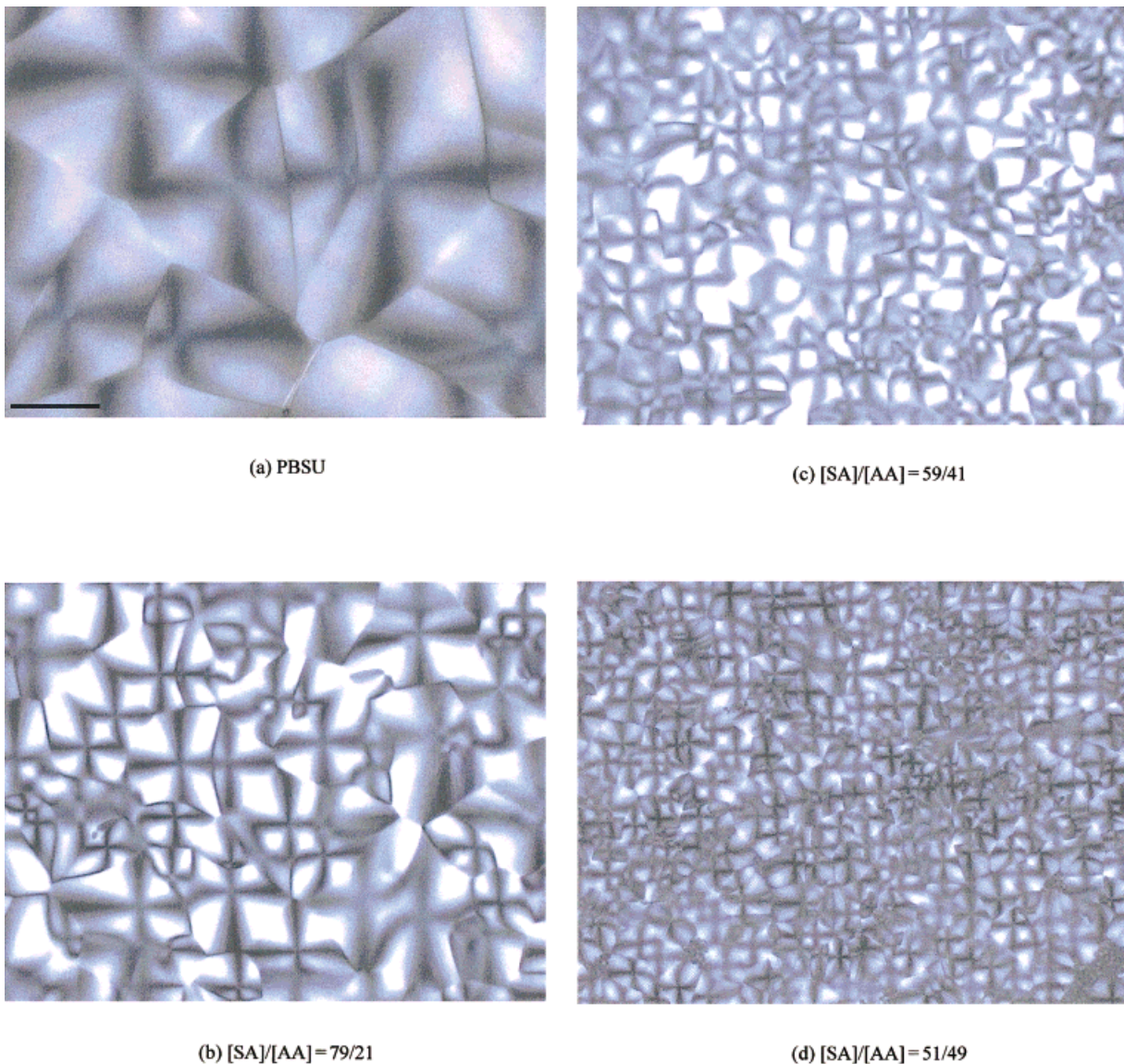


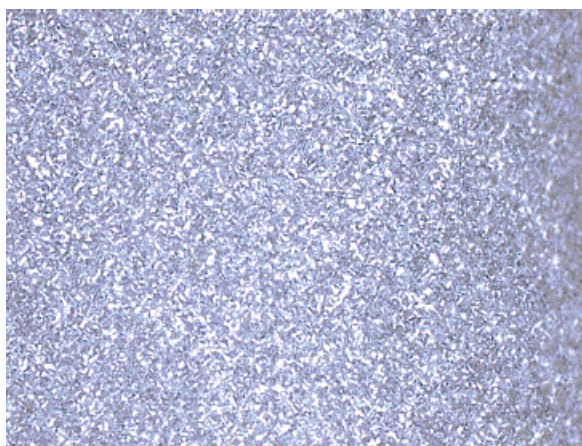
**Figure 8** Polarizing optical micrographs of PBSA copolymers: (a) PBSU, (b) [SA]/[AA] = 79/21, (c) [SA]/[AA] = 59/41, (d) [SA]/[AA] = 51/49, (e) [SA]/[AA] = 38/62, (f) [SA]/[AA] = 20/80, and (g) PBAD. The bar on (a) is 50  $\mu\text{m}$ .

copolyesters are randomly distributed at the copolymer structure, the four methylene groups in the adipate units act as soft segments.<sup>34</sup>

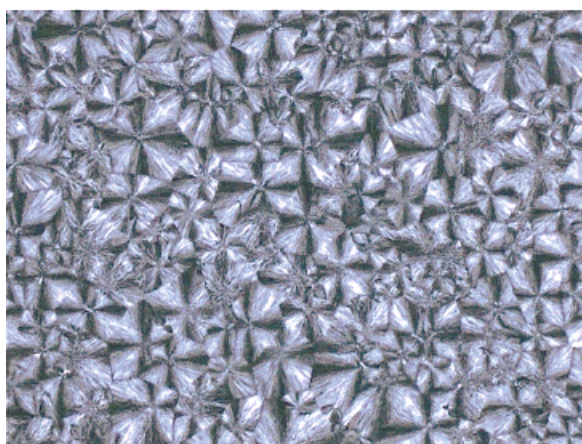
Figure 8 shows the morphology of melt-crystallized isotactic PBSU homopolymer, PBAD homopolymer, and PBSA copolymers.<sup>34,35</sup> They were fused between coverslip and glass slide at the same temperature of 150°C until completely crystallized. The size of PBSU spherulites is observed to be significantly larger than that of PBAD. As the adipate unit of the copolymerization increases, both the crystallinity and the size of spherulite decrease. This can be considered to

be a result of the faster nucleation, which was caused by the copolymerization.

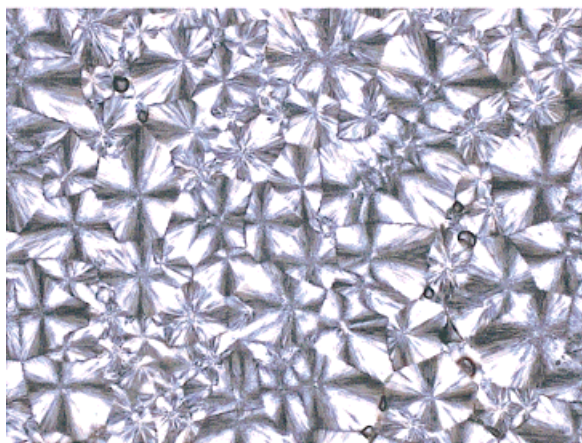
XRD patterns for PBSU homopolymer, PBAD homopolymer, and PBSA copolymers are shown in Figure 9. The crystal unit cell of PBSU is monoclinic and diffraction peaks from [020], [021], and [110] are observed at  $2\theta$  19.4, 21.5, and 22.5°, respectively.<sup>15</sup> The diffraction patterns of PBAD unit at  $2\theta$  value are 21.2, 22.2, and 24.1°, respectively. From the crystal lattice of PBSU, PBAD homopolymer, up to the 51 mol % of succinate composition, the copolymer shows the X-ray diffraction patterns as those of PBSU, whereas the



(c) [SA]/[AA] = 38/62



(f) [SA]/[AA] = 20/80



(g) PBAD

62 mol % of adipate composition shows the diffraction patterns as those of PBAD. Generally, as the ratio of two components of copolymer increases, the XRD pattern is affected by the predominant crystal unit. Therefore, the PBSA 9/1–5/5 composition and PBSA 4/6–1/9 composition are influenced by the diffraction patterns of the PBSU unit and the PBAD crystalline unit. Also, in the XRD pattern for PBSA 5/5 ([SA]/[AA] = 51/49), the diffraction pattern of the succinate unit is more dominant than that of the adipate unit.

As seen in Figure 10, the percentage crystallinity ( $\%X_c$ ) of PBSU homopolymer, PBAD homopolymer, and PBSA copolymers can be obtained by the multiple peak-separation method of X-ray diffraction peak.<sup>36,37</sup> The X-ray diffraction patterns were resolved into crystalline peaks and amorphous peaks by a peak-separation software in XRD. The degree of crystallinity was determined by the area ratio of crystalline peaks and amorphous peaks.<sup>38–40</sup>

In the case of PBSU homopolymer, it consisted of an amorphous peak from the amorphous region and three peaks of [020], [021], and [110] lattices from the diffraction pattern of the crystalline region. After isolating amorphous peaks from the diffraction pattern, the peak areas of each lattice were calculated through peak separation of [020], [021], and [110] lattice of crystalline peaks. The  $\%X_c$  value from the X-ray method was calculated by peak separation of each composition and the  $\%X_c$  value from the DSC method was uniformly divided by the theoretical values of 100% crystalline PBSU and PBAD in Table II and Figure 11. As seen in Figure 11, percentage crystallinity of PBSA copolymers were measured by X-ray and DSC as a function of composition.<sup>41</sup> From the X-ray data, the  $X_c$  value of PBSU homopolymer was 59%, whereas that of PBAD was 43%. As the composition of copolymer increased,  $\%X_c$  of PBSA copolymers decreased between 54 to 32%. The diffraction pattern between PBSU and PBSA 5/5 ([SA]/[AA] = 51/49) was the same as that of the butylene succinate unit, whereas the diffraction pattern between PBAD and PBSA 4/6 ([SA]/[AA] = 38/62) was the same as that of the butylene adipate, as shown in Figure 9. When they are measured by the DSC method, the crystallinity of PBSA copolymers was determined by dividing an observed heat of fusion by the theoretical heat of fusion of PBSU and PBAD without any relation to the composition of copolymers.  $X_c$  values were obtained by dividing the observed

**Figure 8** (Continued from the previous page)

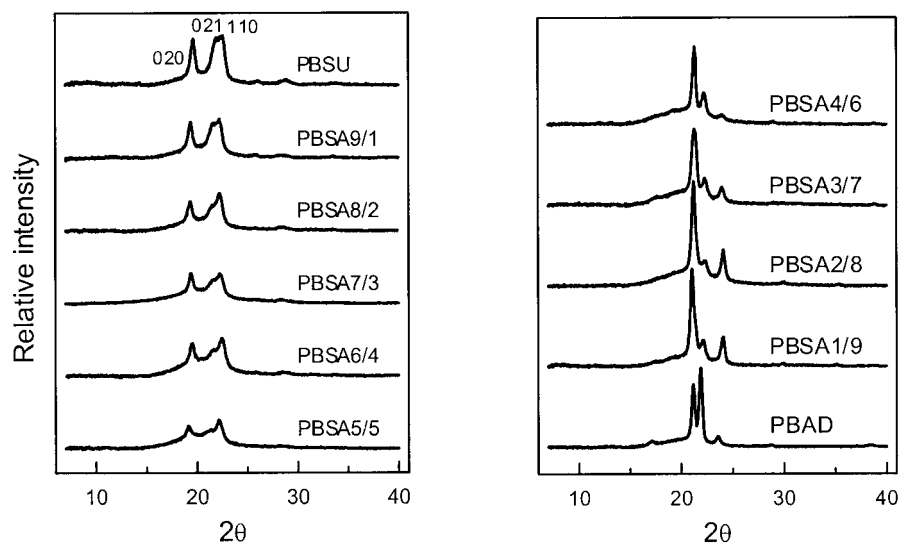


**Figure 9** X-ray diffraction patterns of PBSA copolymers.

heat of fusion from the melting endotherm by the theoretical value (113.4 J/g) for a 100% crystalline PBSU (from PBSU to PBSA 5/5) and by the theoretical value (135.5 J/g) for a 100% crystalline PBAD (from PBAD to PBSA 4/6).<sup>32,42</sup>  $X_c$  values of PBSU and PBAD were 62 and 39%, respectively, from the heat of fusion by DSC. The  $X_c$  values of PBSA copolyesters decreased to between 35 and 25%.

### Polymer Degradation

To investigate the degradation of PBSU homopolymer, PBAD homopolymer, and PBSA co-

polyesters, the experiments on degradation were carried out, respectively, by the biodegradation from microorganisms and by hydrolytic degradation. The degradation test from microorganisms was carried out according to the 301C law (the OECD ready biodegradability guideline) and by the landfill test.

As noted in Figure 12, the organic carbon compound of the sample was degraded into carbon dioxide, water, and energy by microorganisms in the closed system containing activated-sewage sludge. Oxygen was essential for microorganisms in the activated-sewage sludge during degrada-

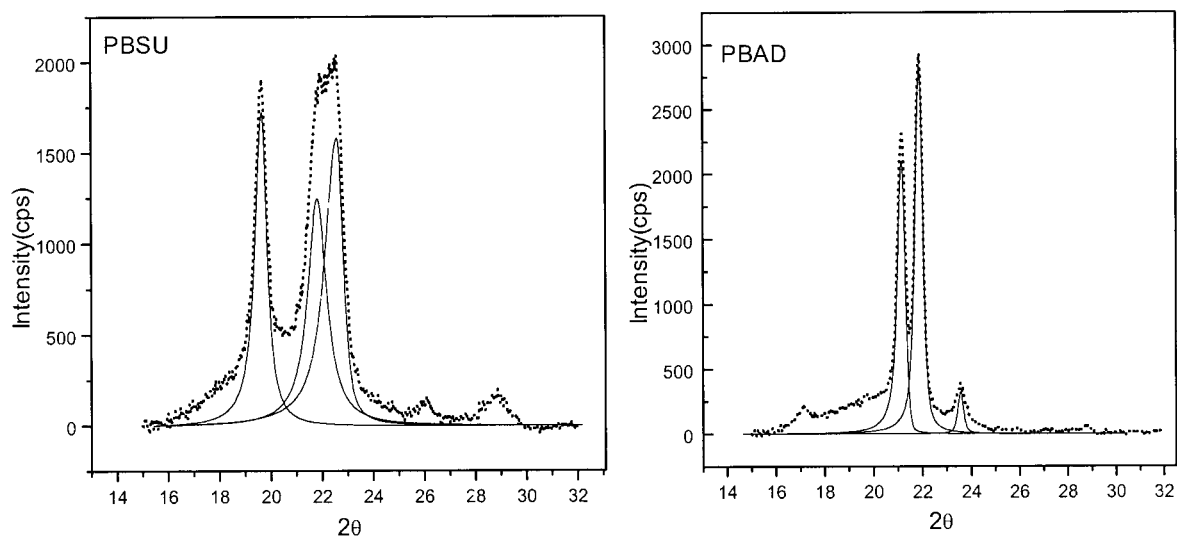


**Figure 10** Peak-separation diagrams of PBSA copolymers by wide-angle X-ray diffraction (WAXD): experimental diffraction peaks (—); crystalline peaks (—) by peak-separation software in XRD.

**Table II Thermal Properties and Percentage Crystallinity of PBSA Copolymers**

Composition Ratio of PBSA Copolyesters <sup>b</sup> [SA]/[AA]	Thermal Properties <sup>a</sup>			Crystallinity	
	$T_m$ (°C)	$T_g$ (°C)	$\Delta H_f$ (J/g)	$X_c$ (%) <sup>c</sup> By DSC	$X_c$ (%) <sup>d</sup> By WAXD
100/0	114	-33	70	62	59
90/10	106	-37	62	55	54
79/21	92	-44	42	37	47
69/31	80	-49	37	33	43
59/41	65	-50	29	26	37
51/49	50	-51	28	25	34
38/62	32	-56	34	25	32
29/71	39	-57	36	27	35
20/80	46	-58	39	29	40
10/90	54	-58	48	35	42
0/100	60	-60	53	39	43

<sup>a</sup> DSC at a heating rate of 10°C/min.

<sup>b</sup> Measured by <sup>1</sup>H-NMR.

<sup>c</sup>  $X_c$  was calculated by dividing the observed heat of fusion from the melting endotherm by the theoretical value (113.4 J/g) for a 100% crystalline PBSU (from 100/0 to 51/49 of polymer composition) and by the theoretical value (135.5 J/g) for a 100% crystalline PBAD (from 38/62 to 0/100 of polymer composition).

<sup>d</sup>  $X_c$  from the X-ray method was calculated by peak separation of each composition.

tion; the biodegradability was measured by the biological oxygen demand (BOD) that was consumed in the closed cultivating reactor. To make the uniform surface area, the sample was dis-

solved in chloroform and poured into cold methanol to make a cottonlike form for usage.

The BOD (in ppm) from the microorganisms increased as the adipate unit of PBSA copoly-

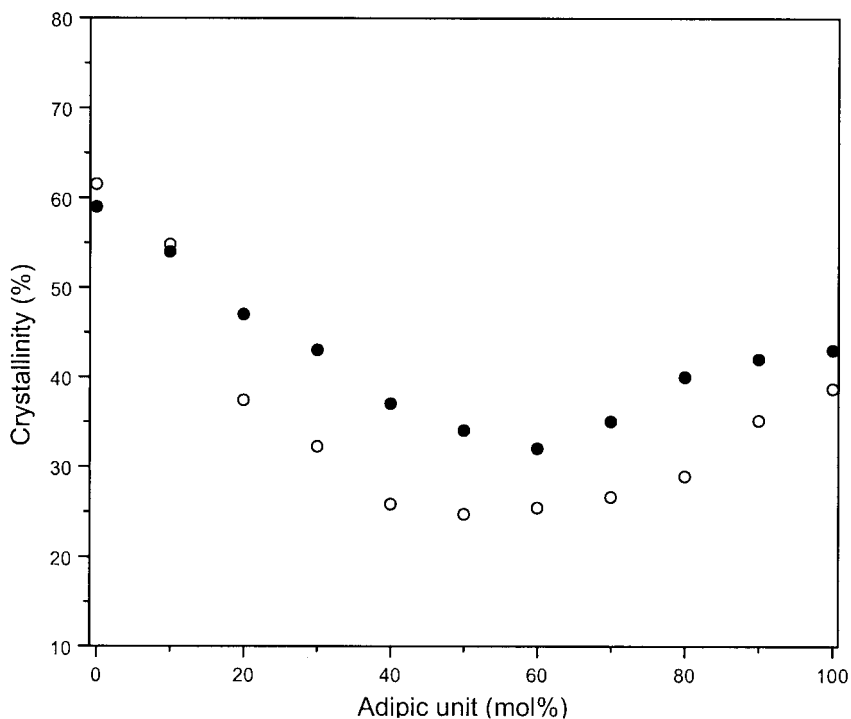


**Figure 11** Percentage crystallinity for PBSA copolymers as a function of composition determined by X-ray (●) and DSC (○).

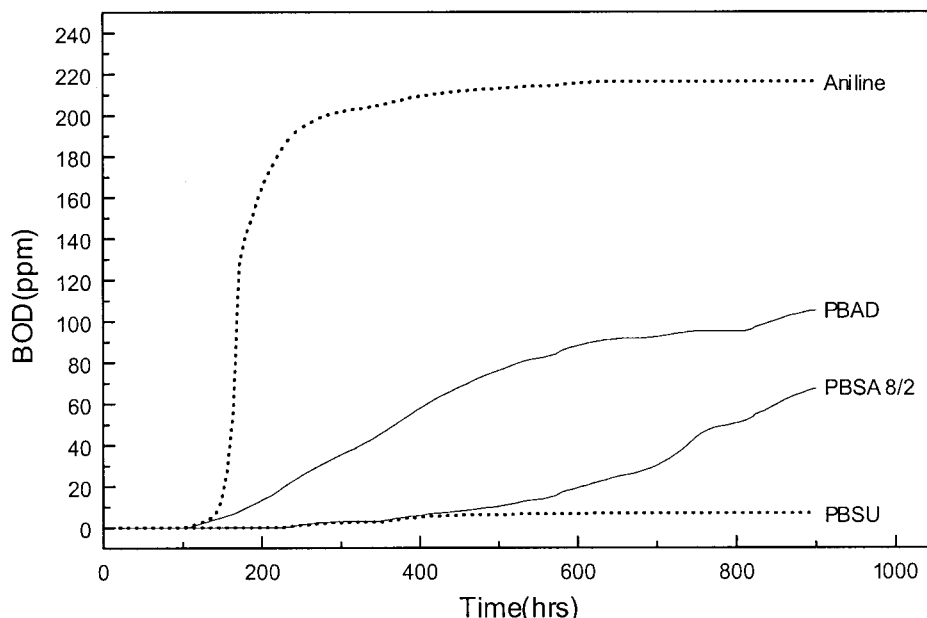


**Figure 12** Biodegradation of the PBSA copolyesters in the closed automatic oxygen supplies system on the activated sludge [OECD guideline for testing of chemicals, ready biodegradability (301C law); sample: solvent-precipitated cotton shape].

ester increased. The quantity of BOD in PBAD homopolymer is quite large compared to that in PBSU homopolymer, which is partially correlated with the crystallinity, the melting point, and the radius of spherulite size in each of the PBSA copolyesters. The degradation data suggest that, although the molecular weight of PBSU homopolymer ( $\bar{M}_n = 7.7 \times 10^{-4}$ ) is lower than that of PBSA 8/2 ( $\bar{M}_n = 9.2 \times 10^{-4}$ ), it is not more degradable. PBSU homopolymer (crystallinity 62%) has a greater degree of crystallinity by 25% than that of PBSA 8/2 copolymer (crystallinity 37%). Furthermore, the spherulite radius of PBSU homopolymer with a spherulite radius of about  $100 \mu\text{m}$  was significantly greater than the radius ( $50 \mu\text{m}$ ) of PBSA 8/2 copolymer.

The relationship between degradability and molecular weights for the two higher molecular weight polymers has not yet been clearly revealed. PBSA 8/2 copolymer was biodegraded to a greater extent than that of PBSU homopolymer, and therefore it shows that the butylene adipate unit provides more factors to be easily attacked by microorganisms than does the butylene succinate unit.<sup>6,11,14,16</sup>

The rate of degradation monitored for PBSU homopolymer, PBAD homopolymer, and PBSA copolyesters revealed the composition depen-

ency. Figure 13 shows the weight loss of the PBSA copolyesters at  $30^\circ\text{C}$  and 90% humidity in the commercial soil (the mixture of 50% compost and 50% soil) for 5 weeks against the copolymer compositions. The degradation rate increased as butylene adipate content increased up to 62 mol %. However, the degradation rate began to decrease with further increase in butylene adipate units. The degradation rate increased as the melting point and crystallinity of PBSA copolymer decreased and the unit of the butylene adipate, rather than butylene succinate, increased. Generally, the susceptibility of a polymer to microbial attack depends on a variety of factors. In addition to the nature of the chemical structure of the polymers, the morphology of the polymer samples greatly affects the rate of biodegradation.

The interesting phenomenon in the landfill test was that the molecular weight of remaining polyester residues from the degradation of microorganisms scarcely changed. Figure 14 shows the weight loss of the PBSA copolymer ( $[\text{SA}]/[\text{AA}] = 79/21$ ) degraded in soil [Fig. 14(a)] and molecular weight change during the degradation [Fig. 14(b)]. From the landfill test, even with 1 to 60% weight loss of film, a change in molecular weight was not monitored.

This phenomenon from the polymer degradation indicates that, unlike the reported low-

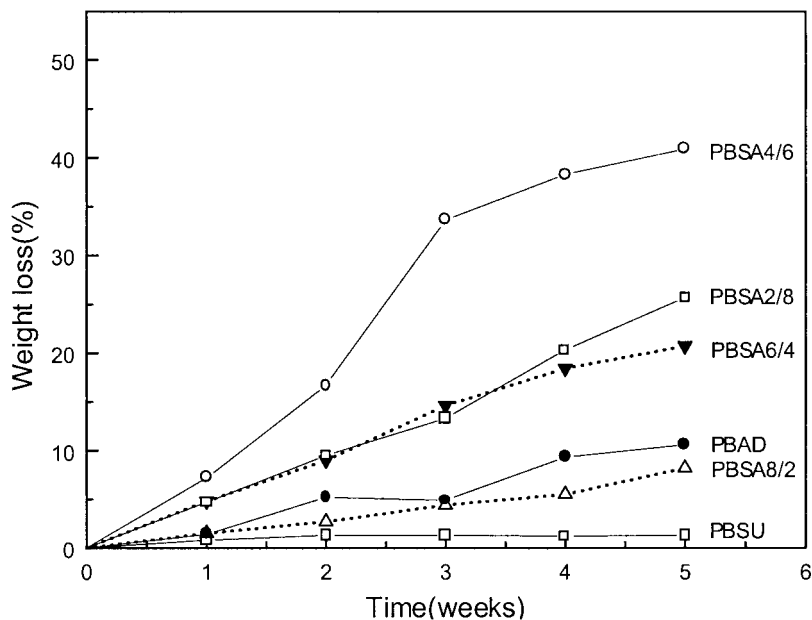
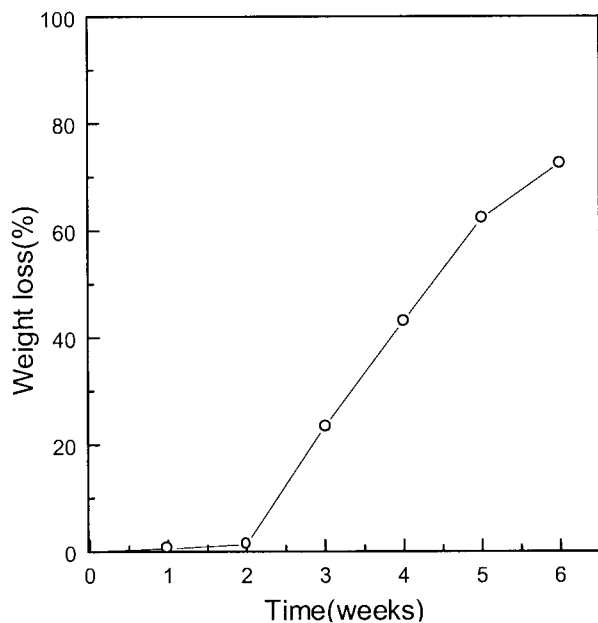


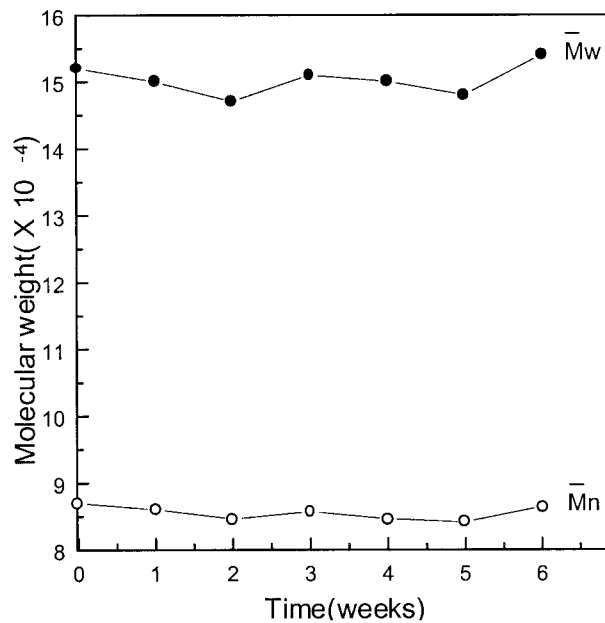
**Figure 13** Weight loss of the PBSA copolyesters degraded at 30°C, 90% humidity in the composting soil (sample: 20 × 20 × 0.4 mm).

molecular polyester, the degradation of high molecular weight PBSU homopolymer, PBAD homopolymer, and PBSA copolyesters by micro-

organisms progresses randomly at the surface of the copolyesters rather than at the main chain scission of polyester.<sup>14,16</sup>

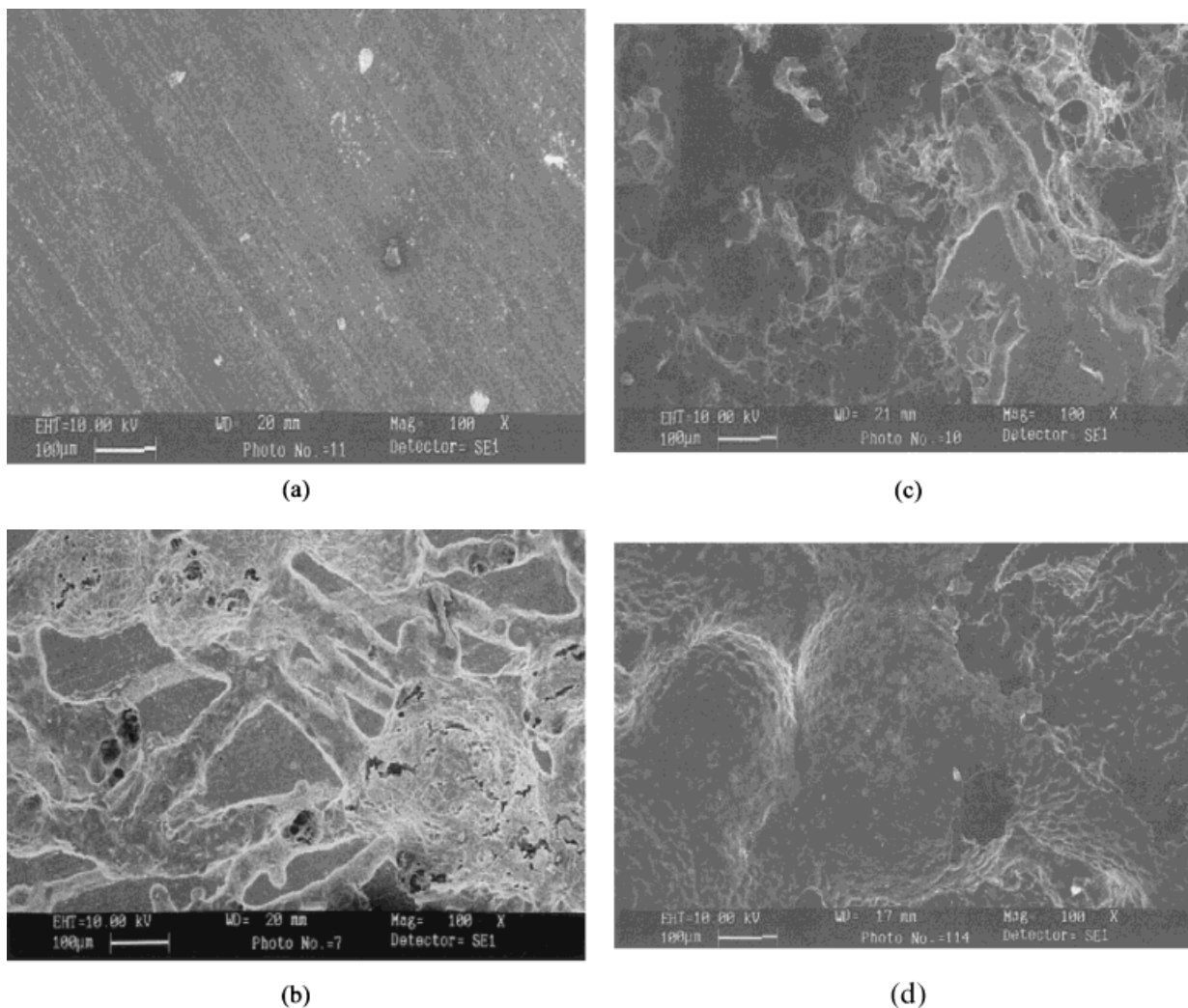


(a)



(b)

**Figure 14** Weight loss of PBSA copolyester ([SA]/[AA] = 79/21): (a) degraded in soil; (b) the molecular weight change during degradation.



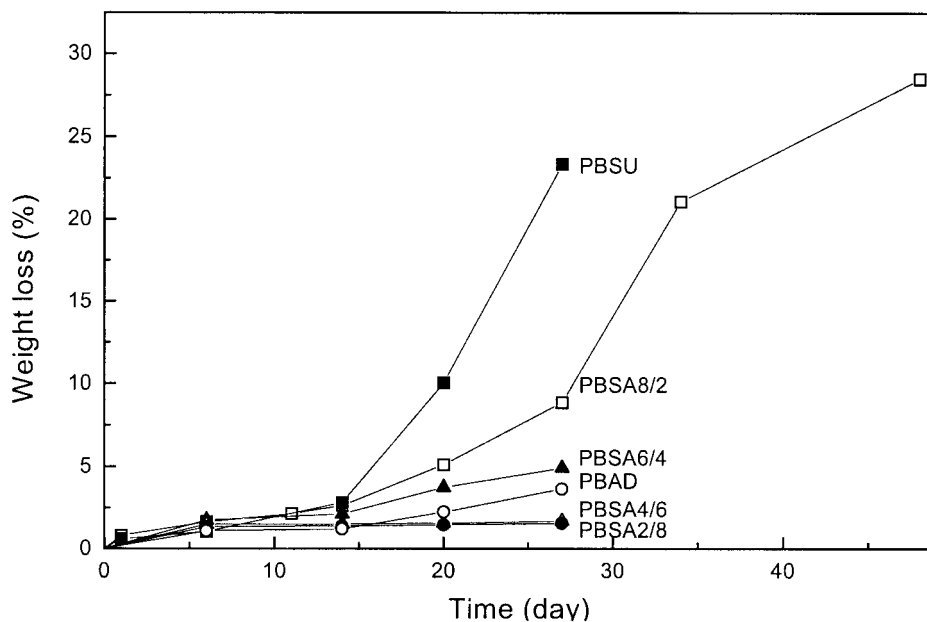
**Figure 15** SEMs of PBSA 8/2 ([SA]/[AA] = 79/21) copolymer film surface after landfill test at 30°C for (a) 2 weeks, (b) 3 weeks, (c) 5 weeks, and (d) 6 weeks.

Figure 15 shows the PBSA 8/2 copolyester ([SA]/[AA] = 79/21,  $\overline{M}_n = 8.7 \times 10^{-4}$ ,  $\overline{M}_w = 15.2 \times 10^{-4}$ ) degraded by 80%. As before, the molecular weight was not observed while the degradation occurs randomly at the polymer surface.

The hydrolytic degradation of PBSU homopolyester, PBAD homopolyester, and PBSA copolyesters was conducted by putting in a melt-press film of 0.4 mm thickness in a test solution (pH 10.6) containing  $\text{NH}_4\text{Cl}$ , ammonia water aqueous solution, and 0.03% of antibacterial agent  $\text{NaN}_3$ . The Erlenmeyer flask was shaken at 30°C in a shaking incubator at a rate of 50 rpm.

The results are shown in Figures 16 and 17, where the weight loss was expressed as a percentage of initial weight and the molecular weight loss of PBSA copolyesters. Figure 18 shows the

scanning electromicrographs of PBSA 8/2 ([SA]/[AA] = 79/21) copolymer films in the course of hydrolytic degradation. At the early stage of hydrolysis, PBSA 8/2 film maintained a smooth surface, although a cracked surface developed at the later stage. Generally, the introduction of a secondary structure in the aliphatic polyesters renders the properties more amorphous and less resistant to the nucleophilic attack to copolyester. In contrast to the hydrolytic degradation of copolyesters, the PBSA copolyesters have a different effect on the hydrolytic degradation. The rate of degradation monitored on PBSA copolyesters revealed a composition dependency. As presented in Figures 16 and 17, the degradation rate decreased as the contents of the adipate unit increased. The presence of butylene adipate units



**Figure 16** Weight loss of PBSA copolymers degraded at 30°C in the ammonium chloride buffer solution ( $\text{NaN}_3$  0.03%, pH 10.6, sample size:  $20 \times 20 \times 0.4$  mm).

may promote the hydrophobic nature of copolyesters, which would negatively influence the hydrolytic susceptibility by sterically hindering the access of nucleophiles. For PBSA copolyesters it appears that the loss of crystallinity became more

critical than the steric hindrance from nucleophiles in the hydrolytic degradation. As shown in Figure 18, SEM photomicrographs on the sample surface during the hydrolytic degradation indicate that there was no change in either the ran-

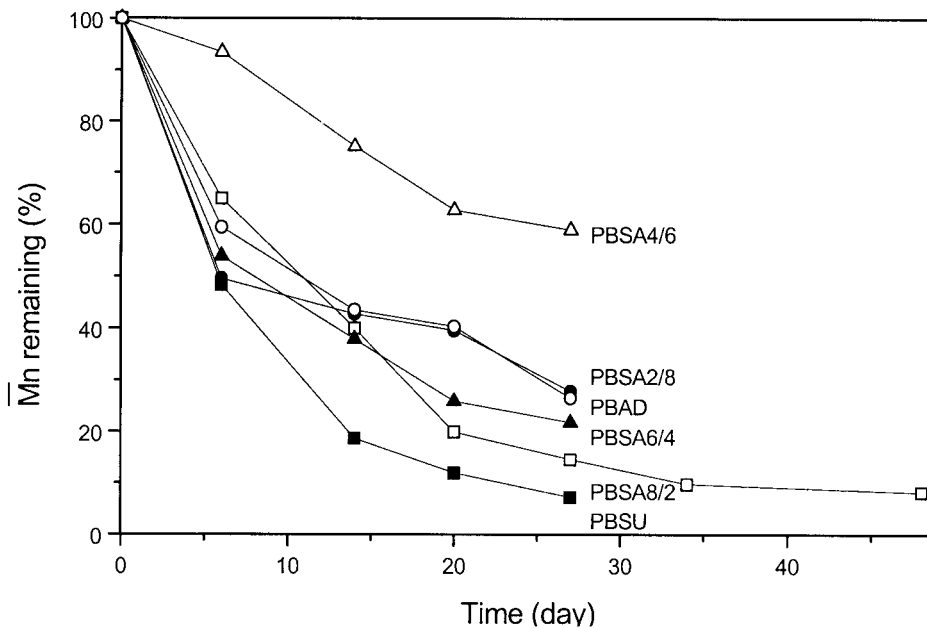


**Figure 17** Number-average molecular weight loss of the PBSA copolymers degraded at 30°C in the ammonium chloride buffer solution ( $\text{NaN}_3$  0.03%, pH 10.6, sample size:  $20 \times 20 \times 0.4$  mm).



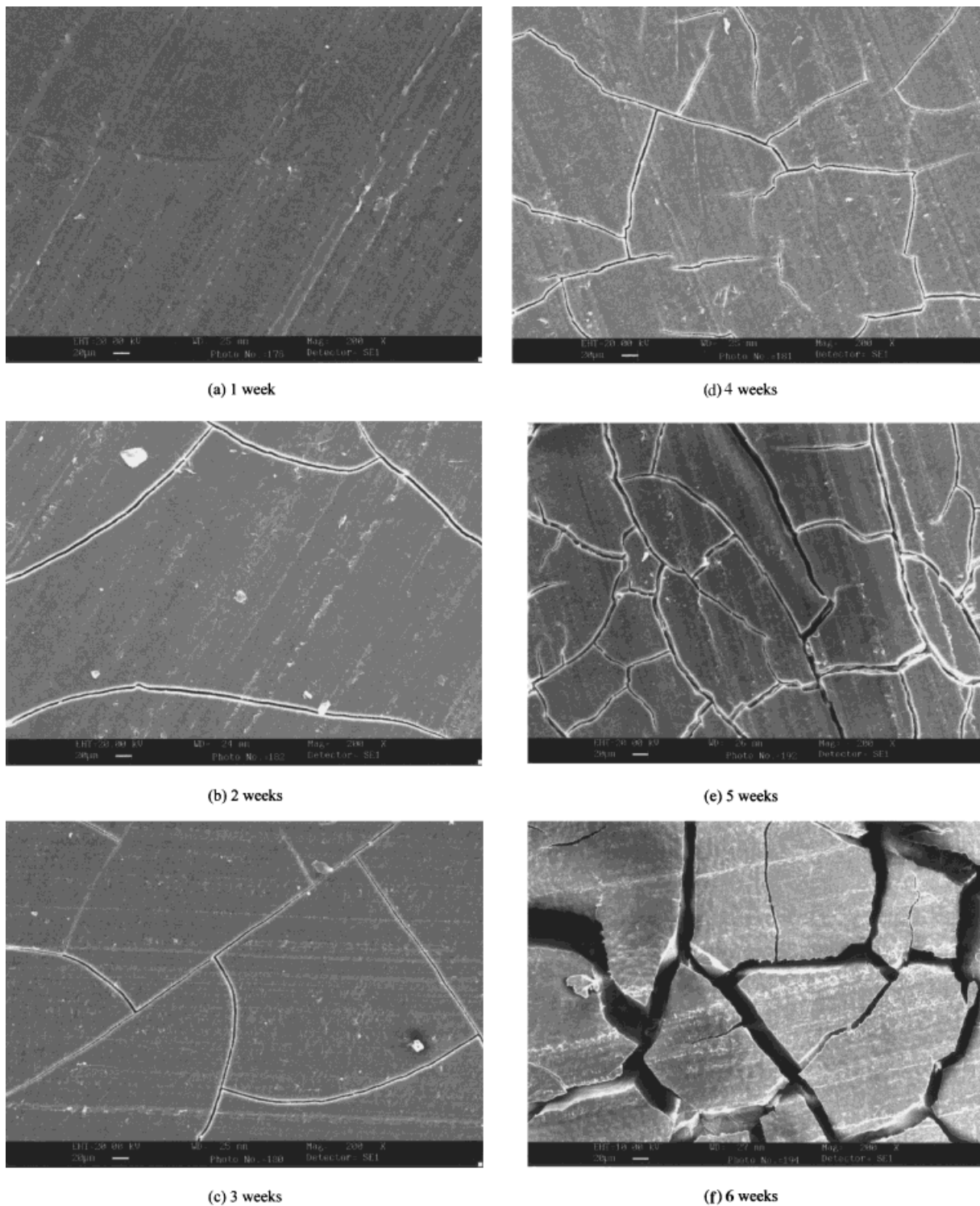


**Figure 18** SEMs of the PBSA 8/2 ( $[SA]/[AA] = 79/21$ ) copolymer film surface after hydrolysis test at 30°C in the ammonium chloride buffer solution ( $\text{NaN}_3$  0.03%, pH 10.6, sample size:  $20 \times 20 \times 0.4$  mm) for (a) 1 week, (b) 2 weeks, (c) 3 weeks, (d) 4 weeks, (e) 5 weeks, and (f) 7 weeks.

dom spatial degradation from microorganisms or the roughness of surface. Furthermore, the images indicate that a hydrated fragment occurred as a result of chain scission. From observing the weight loss of the highly crystalline PBSU homopolymer, PBAD homopolymer, and PBSA copolymers as well as the molecular weight loss, it is certain that the hydrolytic degradation is affected by the alkali solution to a much greater extent than that by the acid solution.

## CONCLUSIONS

Poly(butylene succinate) (PBSU), poly(butylene adipate) (PBAD) homopolymer, and poly(butylene succinate-co-butylene adipate) (PBSA) copolymers were synthesized from succinic acid and adipic acid with 1,4-butanediol by a two-step reaction of esterification and deglycolization. Titanium isopropoxide was used as a catalyst to obtain biodegradable aliphatic polyester that had a higher molecular weight than  $\bar{M}_w$  of 100,000, with narrow molecular weight distributions  $\bar{M}_n/\bar{M}_w$ , which were in the range of between 1.8 and 1.9. The chemical composition of a dicarboxyl unit and 1,4-butanediol unit had a 1 : 1 mol ratio.  $T_g$  and  $T_m$  of PBSU homopolymer were  $-33$  and  $114^\circ\text{C}$ , respectively, and values for PBAD homopolymer were  $-60$  and  $60^\circ\text{C}$ , respectively.  $T_g$  of PBSA copolymers decreased linearly as the adipoyl unit increased. From PBSU homopolymer up to PBSA 5/5 copolymer (adipoyl unit 49 mol %), the melting points decreased and showed a melting endotherm behavior of butylene succinate. Also, as the butylene adipate of copolymer increased from PBSA 4/6 copolymer to PBAD homopolymer, the melting points increased and showed a melting endotherm behavior of butylene adipate. From the observation using the optical polarizing microscope, the radii of spherulites decreased as the adipoyl unit increased. The XRD patterns of homopolymer and copolymer had similar patterns as the DSC melting endotherm changed and showed the diffraction pattern of butylene succinate unit up to PBSA 5/5, and the diffraction pattern of butylene adipate unit from PBSA 4/6. Crystallinity ( $X_c$ ) by DSC decreased to 25% as the chemical composition of the adipate unit became 49 mol %.  $X_c$  values of PBSU homopolymer and PBAD homopolymer from the heat of fusion were 62 and 39%, respectively. To investigate the degradation behaviors of PBSU, PBAD homopolymers, and PBSA copolymers,

the biodegradation and hydrolytic degradation were compared. The biodegradability by microorganisms increased as the contents of butylene adipate increased, along with  $X_c$ ,  $T_m$ ,  $\Delta H_f$ , whereas the spherulite radius decreased. The hydrolytic degradation decreased as the contents of butylene adipate increased. Based on these results, we are now developing the composting package materials of PBSA/poly(ester urethane) block copolymers and pesticide delivery system using PBSA copolymers. Studies of these copolymers are in progress and will be reported shortly.

## REFERENCES

- Gilding, D. K.; Reed, A. M. *Polymer* 1979, 20, 1459.
- Kim, S. H.; Han, Y. K.; Ahn, K. D.; Kim, Y. H.; Chang, T. H. *Makromol Chem* 1993, 194, 3229.
- Pitt, C. G.; Jeffcoat, A. R.; Zweidinger, R. A.; Schindler, A. J. *J Biomed Mater Res* 1979, 13, 497.
- Nakamura, T.; Shimizu, Y.; Takimoto, Y.; Tsuda, T.; Li, Y. H.; Kiyotani, T.; Teramachi, M.; Hyon, S. H.; Nishiya, K. *J Biomed Mater Res* 1998, 42, 475.
- Takiyama, E.; Fujimaki, T. in *Biodegradable Plastics and Polymers*; Doi, Y.; Fukuda, K., Eds.; Studies in Polymer Science; Elsevier Science: Amsterdam, 1994; Vol. 12, p. 150.
- Chen, X.; Gonsalves, K. E.; Cameron, J. A. *J Appl Polym Sci* 1993, 50, 1999.
- Kajikawa, Y.; Yamawaki, K.; Matsuda, A.; Masuda, T. *Polym Prepr (Japan)* 1995, 44, 3186.
- Takiyama, E.; Niikura, I.; Hatano, Y. (to Showa Highpolymer) U.S. Pat. 5,306,787, 1994.
- Takiyama, E.; Niikura, I.; Seki, S.; Fujimaki, T. (to Showa Highpolymer) EU Pat. 565,235 A2, 1993.
- Ratto, J. A.; Stenhouse, P. J.; Auerbach, M.; Mitchell, J.; Farrell, R. *Polymer* 1999, 40, 6777.
- Albertsson, A.-C.; Ljungquist, O. *J Macromol Sci Chem* 1986, A23, 411.
- Nagata, M. *Macromol Rapid Commun* 1996, 17, 583.
- Kanamoto, T.; Tanaka, K. *J Polym Sci A-2* 1971, 9, 2043.
- Song, D. K.; Sung, Y. K. *J Appl Polym Sci* 1995, 56, 1381.
- Ihn, K. J.; Yoo, E. S.; Im, S. S. *Macromolecules* 1995, 28, 2460.
- Albertsson, A.-C.; Ljungquist, O. *J Macromol Sci Chem* 1986, A23, 393.
- Nakafuku, C. *Polym J* 1998, 30, 761.
- Tokiwa, Y.; Suzuki, T. *Nature* 1977, 270, 76.
- Chang, W. L.; Karalis, T. *J Polym Sci* 1993, A31, 493.

20. Kitano, M.; Yakabe, Y. in *Biodegradable Plastics and Polymers*; Doi, Y.; Fukuda, K., Eds.; *Studies in Polymer Science*; Elsevier Science: Amsterdam, 1994; Vol. 12, p. 217.
21. Beigzadeh, D. B.; Sajjadi, S.; Taromi, F. A. *J Polym Sci Part A Polym Chem* 1995, 33, 1505.
22. Kricheldorf, H. R. *Makromol Chem* 1978, 179, 2133.
23. Newmark, R. A. *J Polym Sci Polym Chem Ed* 1980, 18, 559.
24. Yamadera, R.; Murano, M. *J Polym Sci A* 1967, 5, 2259.
25. Hori, Y.; Gonda, Y.; Takahashi, Y.; Hagiwara, T. *Macromolecules* 1996, 29, 804.
26. Fukuzaki, H.; Yoshida, M.; Asano, M.; Aiba, Y.; Kumakura, M. *Eur Polym J* 1990, 26, 457.
27. Nichols, M. E.; Robertson, R. E. *J Polym Sci B* 1992, 30, 305.
28. Nichols, M. E.; Robertson, R. E. *J Polym Sci B* 1992, 30, 755.
29. Cebe, P.; Chung, S. *Polym Compos* 1990, 11, 265.
30. Roberts, R. C. *Polymer* 1969, 10, 117.
31. Todoki, M.; Kawaguchi, T. *J Polym Sci Polym Phys Ed* 1977, 15, 1067.
32. Van Krevelen, D. W. *Properties of Polymers*, 2nd ed.; Elsevier Science: Amsterdam, 1970.
33. Arvanitoyannis, I.; Nakayama, A.; Kawasaki, N.; Yamamoto, N. *Polymer* 1995, 36, 2271.
34. Xhu, L. L.; Wegner, G. *Makromol Chem* 1981, 182, 3625.
35. Norton, D. R.; Keller, A. *Polymer* 1985, 26, 704.
36. Yoshie, N.; Inoue, Y.; Yoo, H. Y.; Okui, N. *Polymer* 1994, 35, 1931.
37. Ruland, W. *Acta Crystallogr* 1961, 14, 1180.
38. Albertsson, A.-C.; Barenstedt, C.; Karsson, S.; Lindberg, T. *Polymer* 1995, 36, 3075.
39. Mohapatra, D. K.; Nayak, P. L.; Lenka, S. *J Polym Sci Polym Chem Ed* 1997, 35, 3117.
40. Joo, Y. L.; Han, O. H.; Lee, H. K.; Song, J. K. *Polymer* 2000, 41, 1355.
41. Roe, R. J.; Gieniewski, C. *J Cryst Growth* 1980, 48, 295.
42. Yoo, Y. T.; Ko, M. S.; Han, S. I.; Kim, T. Y.; Im, S. S.; Kim, D. K. *Polym J* 1998, 30, 538.